



EFFECT OF PARTIAL PRESTRESSING ON CRACKS FOR SIMPLY SUPPORTED POST-TENSION CONCRETE BEAMS

Mohamed Helmy AbdElmageed¹, Tamer Elafandy², Ashraf ElZanaty³

¹PhD Student; ²Professor of Concrete Structures Concrete Institute, Housing and Building National Research Center, Egypt; ³Professor of Concrete Structures Concrete Department Faculty of Engineering, Cairo University, Egypt

ملخص البحث

تمتاز الكمرات مسبقة الإجهاد جزئياً " بقطاعات صغيرة الأبعاد مقارنة بالخرسانة المسلحة النمطية وبالتالي شاع استخدامها وخصوصاً في مجال الكباري ونظراً " لاستخدام قطاعات صغيرة فيعتبر التحكم في الشروخ من أهم محددات التصميم لهذه الكمرات. يقدم هذا البحث دراسة عن الشروخ الناتجة من الأحمال علي الكمرات الخرسانية بسيطة الارتكاز و مسبقة الإجهاد جزئياً والمعرضة لعزوم إنحناء وذلك من خلال عرض الطرق الحسابية بالأبحاث والأكواد المختلفة بالإضافة إلي تسليط الضوء على نتائج الاختبارات السابقة. كما تم عمل برنامج للاختبار المعملية مكون من تسعة كمرات خرسانية مع الأخذ في الاعتبار أن يكون الحد الأقصى للعزوم ثابت علي كل الكمرات مع دراسة تغيير كل من نسب حديد التسليح إلي حديد سبقي الإجهاد وسمك الغطاء الخرساني وعمق حديد سبقي الإجهاد ونسبة حديد التسليح ناحية الضغط. وعلاوة على ذلك تم إنشاء نموذج للكمرات السابقة باستخدام برنامج ANSYS لدراسة مدى توافق شكل الشروخ وتوزيعها مع الاختبار المعملية . بناءً " علي ماسبق تقدم هذه الدراسة اقتراح طريقة لحساب العرض الأقصى للشروخ نتيجة أحمال التشغيل مع الأخذ في الاعتبار تأثير الإجهاد الجزئي المسبق.

ABSTRACT

Advantage of partially prestressed beams is that its cross-section is more slender than traditional reinforced concrete beams; accordingly it is commonly used specially in bridges. Control of cracking is the most important design factor due to usage of this slender concrete section. This paper presents a study of cracking for partially prestressed simply supported concrete beams that are subjected to bending moment. This study is based on formulas stated in different researches and codes. In addition, a program for laboratory tests was created using nine concrete beams, considering a constant moment capacity with variables which are ratios between reinforcement and prestressing steel, concrete cover, eccentricity of prestressing steel and different ratios of compression reinforcement. Moreover, analytical models have been conducted for the previous beams using ANSYS software to confirm cracks pattern and distribution to experimental test. Based on the mentioned studies, a formula has been proposed for calculation maximum crack width due to service loads taking into consideration effect of partial prestressing.

KEYWORDS: Crack width; Ductility; Partial Prestressing; Partial prestressing ratio (PPR); Reinforcing index (w).

1. INTRODUCTION

Cracks under full service loads are allowed in design of partially prestressed concrete consequently studying its effect on durability is considered as one of the main factors of design. Gergely and Lutz (1968) performed statistical analysis on beams and one-way slabs to study flexural crack control based on data for maximum crack width obtained from a number of sources. It was concluded that, tensile stress in steel reinforcement is the most important factor then the thickness of the concrete cover and the area of concrete around each reinforcing bar. Other factors also affect crack width but are not major factors like the bar diameter and the ratio of the strain at the concrete surface to strain at reinforcement level [10]. For partially prestressed concrete, crack width calculation is more complicated than non-prestressed concrete because it should be performed in two steps. First, the decompression stress is calculated which cause zero stress at prestressing steel level; second the increase of stresses after this point is the stresses considered in crack width calculation as a non-prestressed element. Many formulas have been stated for calculation of crack width based on those factors.

This paper presents a formula to calculate crack width taking into consideration effect of partially prestressing based on results of experimental investigation developed to assess the behavior of partially prestressed beams with different ratio of partially prestressing, concrete cover, compression reinforcement ratio and eccentricity of prestressing steel. The experimental program is composed of nine beams with constant moment capacity and in the remaining sections of this paper; the experimental program will be thoroughly discussed. In addition, analytical models were created by using ANSYS software for checking cracks pattern and distribution only due to difficulty to obtain accurate crack width by using this model. Also results of a previous experiment by A.E. Namman and M.H. Harajli [7] has been reported and compared versus proposed formula. Analytical models and previous experiments indicated that results are very close to that conducted in the laboratory and the proposed formula.

2. Experimental Work and Results

2.1. Beams Properties and Variables

The experimental program is composed of nine simply supported partially prestressed concrete beams considering a constant ultimate resistance in flexure.

Beams dimensions were 300mm width, 450mm overall depth and 4680mm clear span; the 28-days cube compressive strength was 38.5 Mpa. All non-prestressed reinforcement had yield strength of 489 Mpa and ultimate strength of 630 Mpa. On the other hand, prestressing steel were 15.24mm and 12.7mm, and the yield/ultimate strength were 1765/1940 Mpa and 1840/1980 Mpa respectively. The stirrups for all beams were 10mm diameter bars every 200mm at mid-span and 100 at beam ends with a volumetric percentage of 0.40% at mid-span and 0.80% at beam ends. End plate has been erected at each beam ends to enhance distribution of anchor stress on concrete section. In addition, spiral ties 12mm diameter bar with 50mm pitch for a 500mm distance was fixed at ends to resist thrust force. Fig.1 illustrates detailed dimensions of all beams. The profile of

prestressing steel is trapezoidal erected inside a corrugated polyethylene duct 25mm diameter with two tubes for grouting at distance 600mm from beam ends.

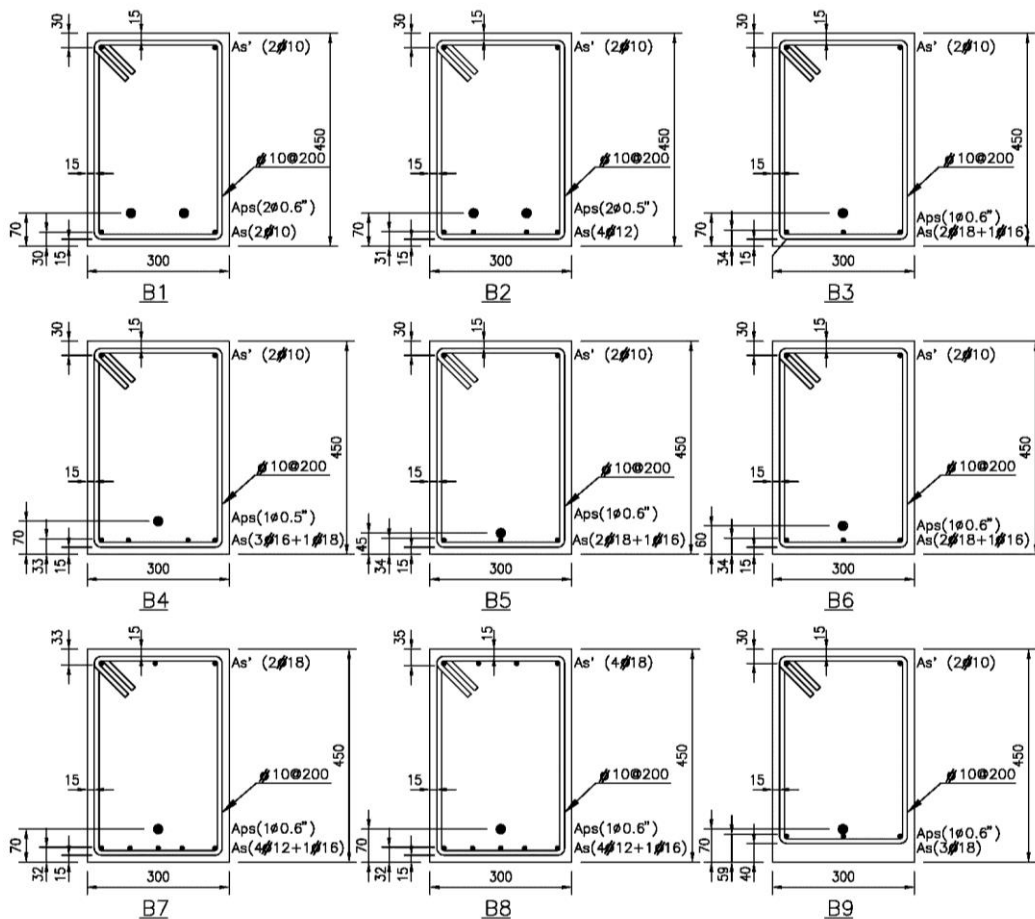
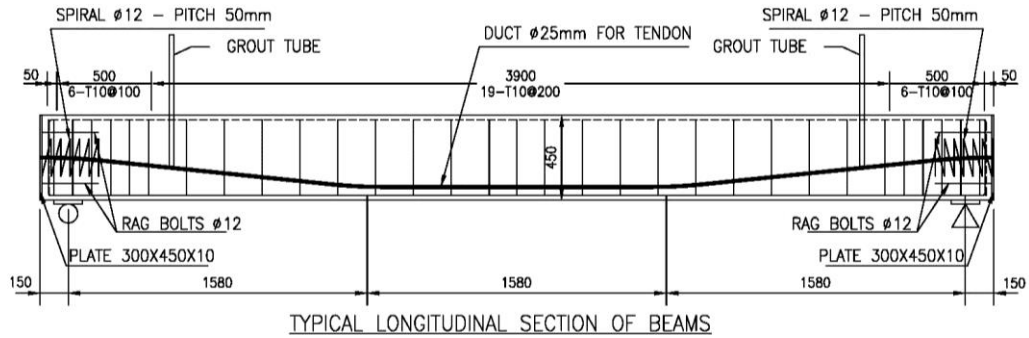


Figure 1: Tested beams details and sections

Variables are partial prestressing ratio PPR ($PPR = \frac{M_{ult. \text{ of pres. steel}}}{M_{ult. \text{ of pres. steel} + R_{ft}}$), depth of prestressing steel, compression reinforcement ratio and concrete cover; as shown in Table 1. Four beams had different PPR which is the most important variable of this study, whereas PPR equal 0.86, 0.61, 0.41 and 0.29 assigned for beams B1, B2, B3 and B4 respectively, while remaining beams have PPR close to partial prestressing ratio of beam B3; all eccentricities of prestressed steel were 155mm except for B5 and B6 were 180mm and 165mm respectively; compression reinforcement was 157mm² for all beams except for B7 and B8 were 508mm² and 1016mm² respectively. Cover of reinforcement was 50mm for B9 while it was 25mm for all other beams.

Table 1: Beams variables

| BEAM | A _{ps} mm ² | A _s mm ² | A _s ' mm ² | d _p mm | d mm | d' mm | cover mm | Partial Prestressing ratio PPR |
|------|------------------------------------|-----------------------------------|-------------------------------------|----------------------|---------|----------|-------------|--------------------------------------|
| B1 | 280 (2Ø0.6") | 157 (2T10) | 157 (2T10) | 380 | 420 | 30 | 25 | 0.86 |
| B2 | 197.4 (2Ø0.5") | 452 (4T12) | 157 (2T10) | 380 | 419 | 30 | 25 | 0.61 |
| B3 | 140 (1Ø0.6") | 709 (1T16+2T18) | 157 (2T10) | 380 | 416 | 30 | 25 | 0.41 |
| B4 | 98.7 (1Ø0.5") | 857 (3T16+1T18) | 157 (2T10) | 380 | 417 | 30 | 25 | 0.29 |
| B5 | 140 (1Ø0.6") | 709 (3T18) | 157 (2T10) | 405 | 416 | 30 | 25 | 0.41 |
| B6 | 140 (1Ø0.6") | 709 (1T16+2T18) | 157 (2T10) | 390 | 416 | 30 | 25 | 0.41 |
| B7 | 140 (1Ø0.6") | 653 (4T12+1T16) | 508 (2T18) | 380 | 418 | 34 | 25 | 0.43 |
| B8 | 140 (1Ø0.6") | 653 (4T12+1T16) | 1016 (4T18) | 380 | 418 | 34 | 25 | 0.43 |
| B9 | 140 (1Ø0.6") | 762 (3T18) | 157 (2T10) | 380 | 391 | 30 | 50 | 0.38 |

2.2. Prestressing Losses

Prestressing force was applied from both ends in five steps consecutively, start by 25% from 1st end then 50% from 2nd end, 75% from 1st end, 100% from 2nd end and last 100% from 1st end. Losses due to friction and seating of anchors are 20.5% for B2 and B4; while losses are 24.5% for other beams as shown in Fig 2 and Fig 3. B1 and B2 had additional losses due to elastic shortening of concrete 1.5% (20.3 Mpa) and 1% (15.2 Mpa) respectively. In addition, long term losses are also calculated (based on guidelines of reference [1], [8] and [9]) due to the duration between prestressing and loading time, and it

had a minimal effect about 1% because of short duration with a maximum one month. Table 2 shows summary of losses for each beam.

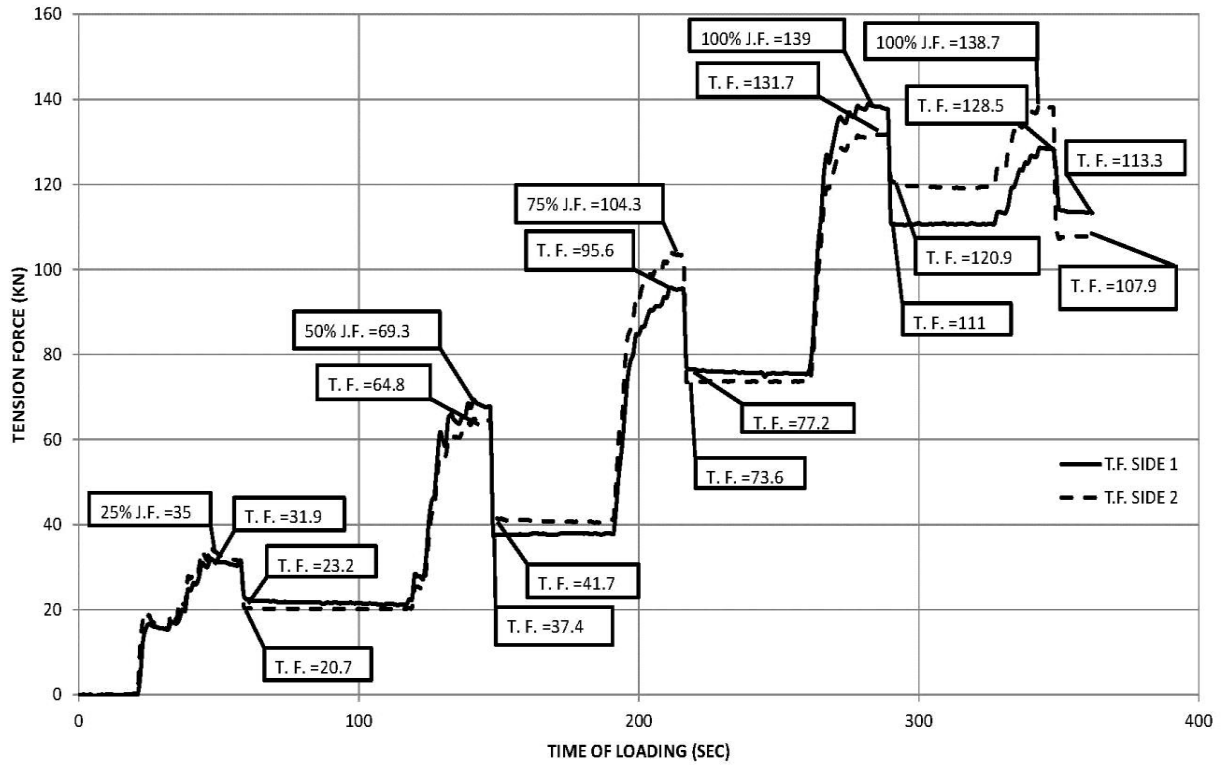


Figure 2: Losses at transfer stage in Group 1- tendon 0.5"

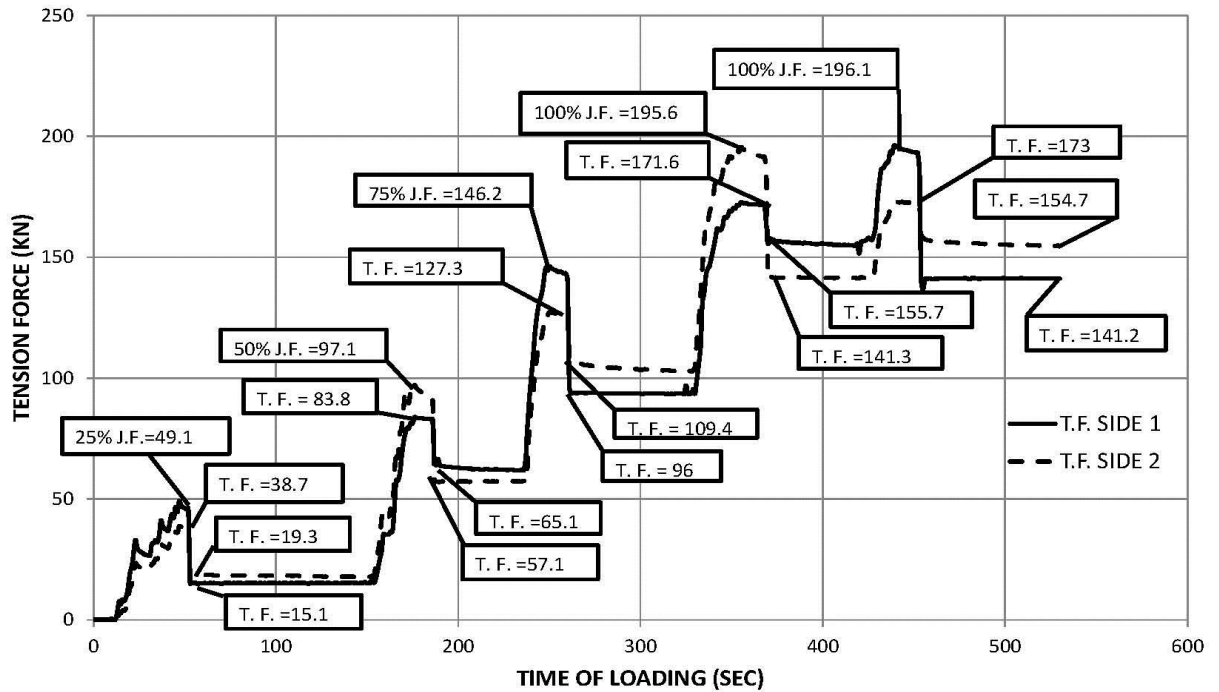


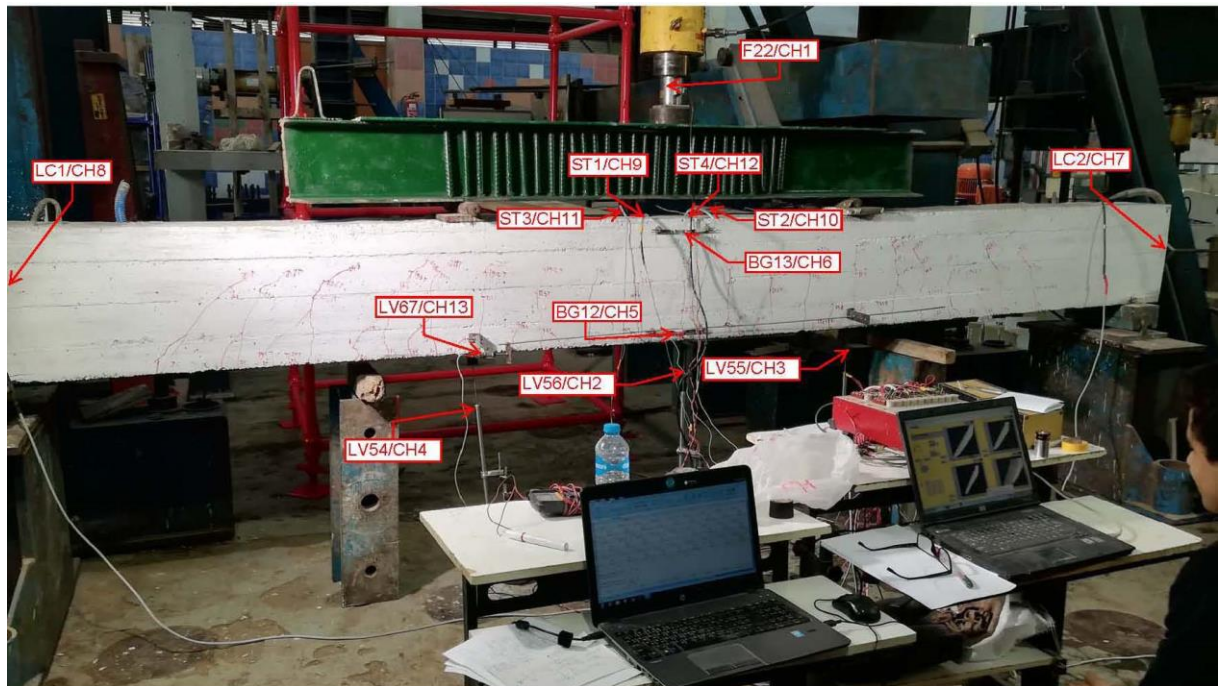
Figure 3: Losses at transfer stage in Group-2 tendon 0.6"

Table 2: Beams Losses

| BEAM | Transfer Losses (Mpa) | | | Long Term Losses (Mpa) | | | Total Losses (Mpa) | Total Losses (%) |
|------|-----------------------|---------|--------------------|------------------------|----------------|------------------|--------------------|------------------|
| | Friction | Seating | Elastic shortening | Concrete Shrinkage | Concrete Creep | Steel relaxation | | |
| B1 | 168.2 | 173.9 | 20.3 | 1.8 | 5.5 | 2.8 | 372.5 | 26.6 |
| B2 | 88.7 | 197.6 | 15.2 | 4.2 | 4.1 | 4 | 313.8 | 22.3 |
| B3 | 168.2 | 173.9 | 0 | 8.1 | 2.9 | 3.3 | 356.4 | 25.5 |
| B4 | 88.7 | 197.6 | 0 | 2.3 | 2 | 3.6 | 294.2 | 20.9 |
| B5 | 168.2 | 173.9 | 0 | 5.3 | 3.1 | 2.9 | 353.4 | 25.3 |
| B6 | 168.2 | 173.9 | 0 | 1.5 | 2.7 | 2.5 | 348.8 | 24.9 |
| B7 | 168.2 | 173.9 | 0 | 0.8 | 2.7 | 2.4 | 348 | 24.9 |
| B8 | 168.2 | 173.9 | 0 | 1.9 | 2.7 | 2.8 | 349.5 | 25.0 |
| B9 | 168.2 | 173.9 | 0 | 3 | 3 | 2.7 | 350.8 | 25.1 |

2.3. Test Setup

Fig. 4 shows the test set-up where beams were simply supported on hinged and roller supports at 150mm from both beam ends.



ST1 : BOTTOM STRAIN GAUGE (FRONT SIDE)
 ST3 : TOP STRAIN GAUGE (FRONT SIDE)
 BG12: BOTTOM BI GAUGE
 LV54: VERTICAL LVDT UNDER LEFT LOAD
 LV56: VERTICAL LVDT UNDER RIGHT LOAD
 LC1: LOAD CELL AT LEFT END
 F22: APPLIED FORCE

ST2: BOTTOM STRAIN GAUGE (BACK SIDE)
 ST4 : TOP STRAIN GAUGE (BACK SIDE)
 BG13: TOP BI GAUGE
 LV55: VERTICAL LVDT UNDER MIDDLE OF BEAM
 LV67: HORIZONTAL LVDT BETWEEN LEFT AND RIGHT LOADS
 LC2: LOAD CELL AT RIGHT END

Figure 4: Test set-up

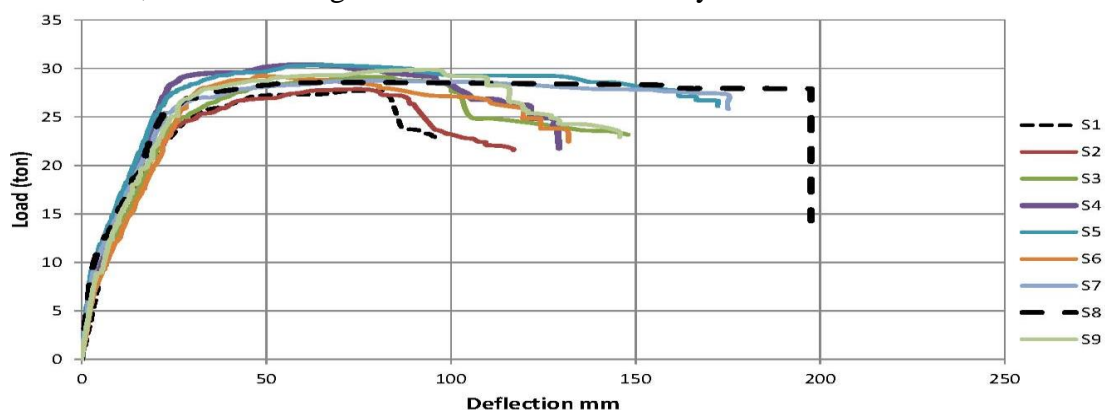
The beams have been tested under loads till flexure failure. A hydraulic machine of capacity 500 KN has been used on top of stiffened steel I beam that transfer loads to two points on top of concrete beam spaced 1580mm at middle third of clear span. Stroke control system had been used to control deflection increment during applying load where increment starts with 0.5mm till reaching deflection 4mm, then increments increase gradually to be 1mm, 1.5mm, 2mm and 3mm till achieving deflection 10mm, 20mm, 45mm and 60mm respectively; and finally increment is 5mm till failure. At end of each loading cycle crack width, length and spacing were recorded. Also, strain at top and bottom reinforcement was measured using four electric strain gauges fixed with top and bottom reinforcement. In addition, horizontal linear variable differential transducers (LVDT) were erected on one side of beam and 40mm above bottom level. On the other hand, vertical deflection was measured at middle of beam and under the two concentrated loads by using three linear variable differential transducers (LVDT). All data from previous instrumentations and from load cell under hydraulic machine have been collected through a data acquisition system and software “Lab view”.

2.4. Test Results

The Nine beams were tested till failure, and a comparison between beams ductility is shown in Fig. 5 and it has been found that beam S1 had lower ductility due to high value of its PPR, while beam S8 had the higher ductility (around 2.3 times of S1 ductility) resulting from lower PPR and maximum compression reinforcement comparing with other tested beams.

Failures of all tested beams were ductile failures as shown in Fig. 6. A comparison was developed between deflection from laboratory test results and calculation based on moment-curvature curve (refer to Fig. 7) which indicates acceptable results.

In addition, a comparison between actual and estimated cracking-load, yield-load and ultimate load were presented in Table 3; it is clear that calculation for yield-load and ultimate load are very close to actual values with maximum difference ranging between 0% and 13%; while cracking-load indicates less accuracy with maximum difference of 8%.



| Beam | S1 | S2 | S3 | S4 | S5 | S6 | S7 | S8 | S9 |
|-----------|-----|-----|-----|-----|-----|-----|-----|-----|-----|
| Ductility | 3.6 | 4.3 | 5.5 | 4.8 | 6.4 | 4.9 | 6.5 | 7.3 | 5.4 |

Figure 5: Load-deflection and ductility comparison between tested beams

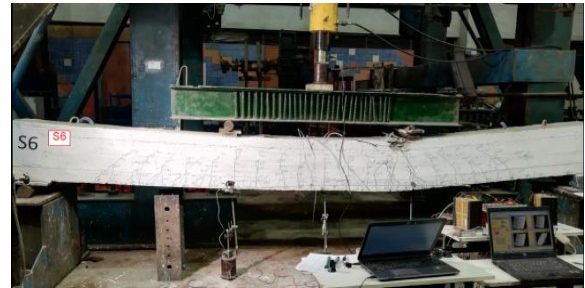
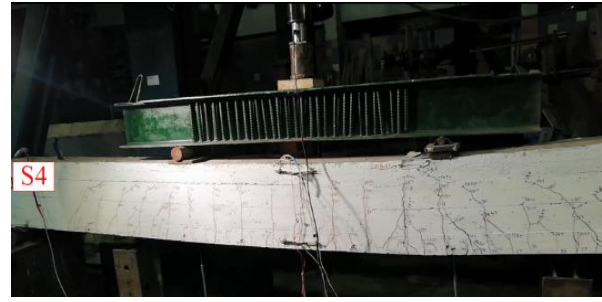


Figure 6: Failure modes (ductile) for tested beams

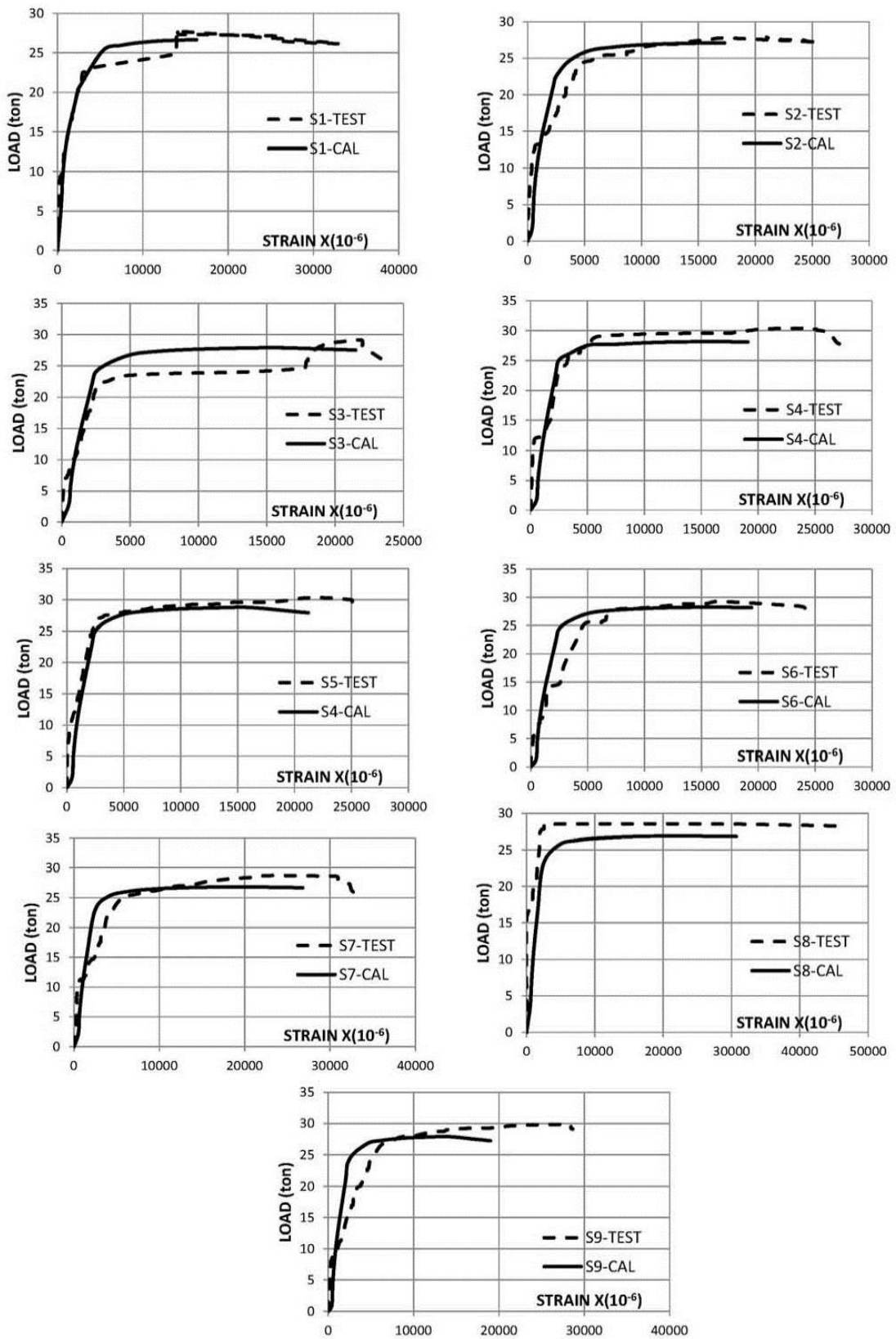


Figure 7: Load-Strain comparison between Lab. test results and Analytical study

Table 3: Comparison between actual-loads and estimated-loads

| Beam | Cracking load (ton) | | | Yield load (ton) | | | Ultimate load (ton) | | |
|------|---------------------|-------|----------|------------------|-------|----------|---------------------|-------|----------|
| | Test | Cal. | Test/Cal | Test | Cal. | Test/Cal | Test | Cal. | Test/Cal |
| S1 | 12.70 | 12.13 | 1.05 | 22.4 | 20.49 | 1.09 | 27.72 | 26.65 | 1.04 |
| S2 | 11.40 | 10.12 | 1.13 | 23.38 | 22.39 | 1.04 | 27.87 | 27.09 | 1.03 |
| S3 | 8.3 | 8.09 | 1.03 | 22.10 | 23.94 | 0.92 | 29.14 | 27.89 | 1.04 |
| S4 | 6.90 | 7.09 | 0.97 | 23.13 | 24.96 | 0.93 | 30.39 | 28.16 | 1.08 |
| S5 | 9.80 | 8.59 | 1.14 | 26.17 | 24.84 | 1.05 | 30.30 | 28.76 | 1.05 |
| S6 | 8.80 | 8.30 | 1.06 | 25.00 | 24.96 | 1.00 | 29.25 | 28.16 | 1.04 |
| S7 | 9.50 | 8.23 | 1.15 | 22.10 | 22.89 | 0.97 | 28.74 | 26.82 | 1.07 |
| S8 | 9.60 | 8.45 | 1.14 | 25.97 | 23.02 | 1.13 | 28.53 | 26.89 | 1.06 |
| S9 | 8.60 | 8.00 | 1.08 | 23.97 | 24.23 | 0.99 | 29.84 | 27.90 | 1.07 |

Fig. 8 shows the major effect of PPR on crack width at service load stage of the tested beams. It is clear that PPR is inversely proportioned with crack width within service load range but at the maximum service load crack width is almost has the same value. Also it shows the effect of PPR in first crack load where increasing PPR from 0.29 to 0.86 caused increasing of first crack load by twice of its value.

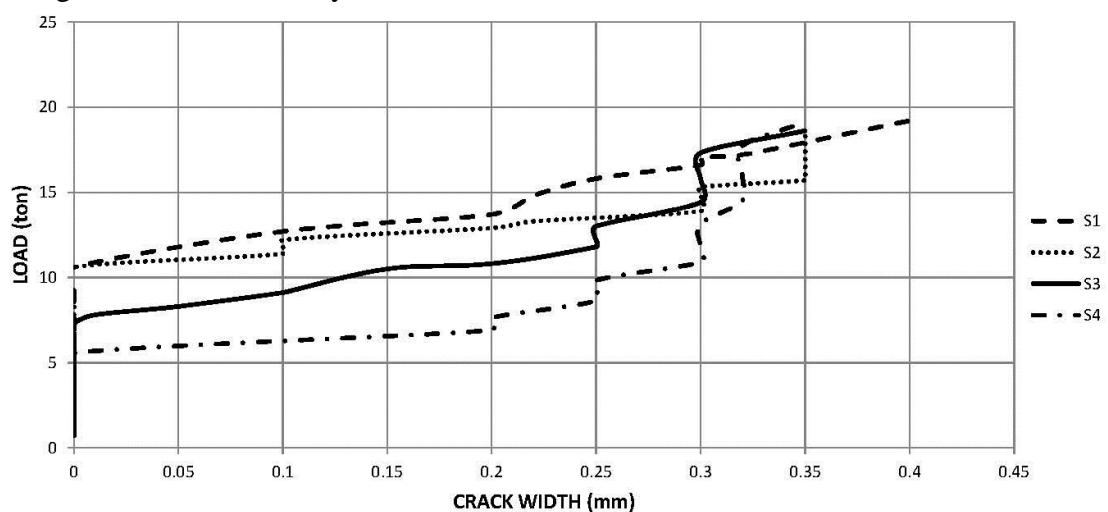


Figure 8: Comparison of tested beams crack width with variable PPR

Also, increasing depth of prestressing by 7% increased crack width at maximum service load level by 17% as shown in Fig. 9; thus due to increasing compression stresses near bottom of beam resulting from increasing moment of prestressing.

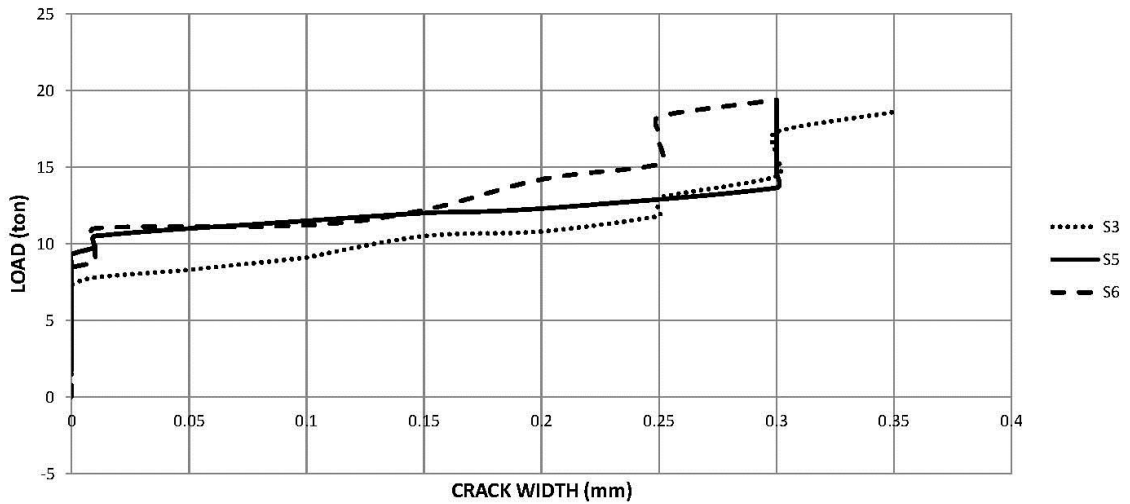


Figure 9: Comparison of tested beams with variable d_p

Fig. 10 shows effect of compression reinforcement where increasing A_s' from 0.116% to 0.377% caused enhancement in crack width by 17%; while increasing A_s' from 0.753% to 1.25% is not effective at maximum service load.

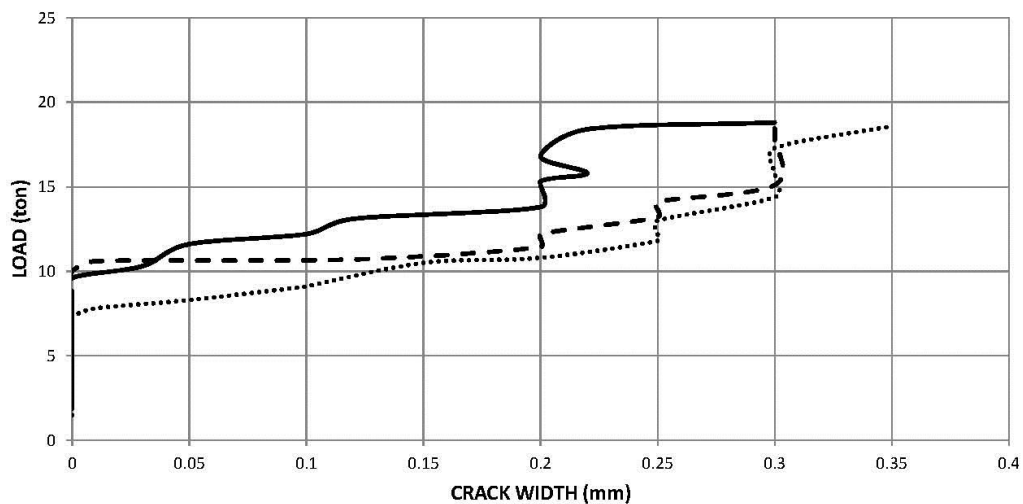


Figure 10: Comparison of tested beams with variable A_s'

On the other hand, concrete cover has a major effect as shown in Fig. 11 especially at maximum service load whereas crack width increase by 33% due change cover from 25mm to 50mm.

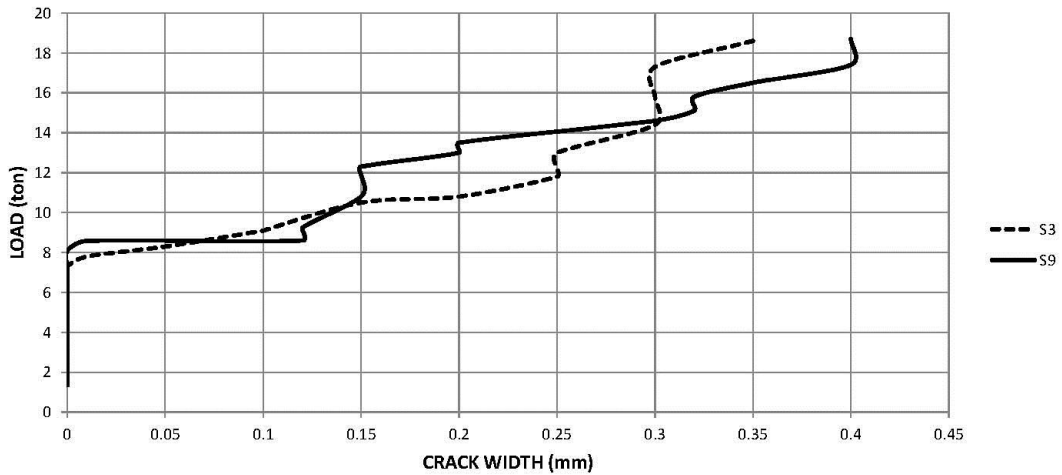


Figure 11: Comparison of tested beams with variable concrete cover

A comparison between cracks width, spacing and length was conducted as shown in Table 4; it is clear that PPR is the most effective on cracking behavior were increasing of PPR caused minimizing of both number of cracks and average crack width with maximum spacing between cracks; while its maximum crack width has a large value of 0.4mm. Also concrete cover minimizes number of cracks with maximum spacing but it did not enhance average width of cracks or maximum crack width. On the other hand, using PPR ratio around 0.4 enhanced maximum crack width to be 0.30mm instead of 0.40mm results from PPR 0.86 and thus due to increase area of reinforcement bars (reducing tensile stresses) near tension side but it caused increasing of number of cracks comparing with higher values of PPR.

Table 4: Comparison of Cracks within service load range

| Beam | Number of Cracks | Crack Width | | Crack Length | | Crack Spacing | |
|------|------------------|--------------------|--------------------|---------------------|---------------------|----------------------|----------------------|
| | | Average Width (mm) | Maximum Width (mm) | Average Length (mm) | Maximum Length (mm) | Average Spacing (mm) | Maximum Spacing (mm) |
| S1 | 16 | 0.16 | 0.40 | 216 | 306 | 123 | 230 |
| S2 | 25 | 0.26 | 0.40 | 178 | 325 | 102 | 190 |
| S3 | 35 | 0.20 | 0.35 | 177 | 329 | 86 | 150 |
| S4 | 29 | 0.16 | 0.32 | 177 | 363 | 91 | 195 |
| S5 | 19 | 0.18 | 0.30 | 199 | 300 | 101 | 205 |
| S6 | 28 | 0.15 | 0.30 | 173 | 311 | 78 | 160 |
| S7 | 27 | 0.14 | 0.30 | 179 | 318 | 91 | 180 |
| S8 | 34 | 0.12 | 0.30 | 169 | 388 | 85 | 165 |
| S9 | 20 | 0.22 | 0.40 | 224 | 370 | 122 | 200 |

3. Analytical Model and Previous tests by A.E. Namman and M.H. Harajli [7]

3.1. Analytical Model

A 3D-model has been performed using ANSYS software to simulate the experimental test and check crack pattern and distribution. Concrete was modeled using Solid 65 material solver, steel and tendons were modeled using Link 180 material solver, mesh was chosen to be boxes (solid parts and link members) with max dimension of 50 mm, which was found as suitable as reducing mesh to 25mm resulting in less than 2% with solving time of 6 multiples. Boundary limits were chosen to simulate the experiment, with mid-span axis of symmetry (solving half model). Loads are assigned on a steel plate with dimension 300*100*20 mm resting on the concrete, with bottom support of line restricted to move down but allowed to rotate (hinged support).

3.1.1. Comparison between experimental tests and analytical model

Cracks zone results from the analytical models were verified with corresponding results of experimental tests refer to Fig. 12.



Figure 12: crack zone comparison of analytical and experimental results.

3.2. Results of previous tests by A.E. Namman and M.H. Harajli [7]

In 1984, Harajli and Naaman studied the effect of fatigue resistance of partially prestressing concrete beams by testing twelve sets of beams. Each set consisted of two identical beams; first beam subjected to cyclic load, and the second beam subjected to static load. The main variables for the twelve sets were the partial prestressing ratio (PPR) which varied as 0.0, 0.33, 0.67 and 1.0; and the reinforcing index ($\tilde{\omega}$) which varied between $\tilde{\omega}_{max}$, $\frac{2}{3}\tilde{\omega}_{max}$ and $\frac{1}{3}\tilde{\omega}_{max}$. Each set consisted of two beams; first subjected to static load till the ultimate load while the second subjected to cyclic load between 40% and 60% from the maximum static load. Fig. 13 show beams properties. This study highlights results of the partial prestressed beams only which is indicated as PP1-S1, PP1-S2, PP1-S3, PP2-S1, PP2-S2 AND PP2-S3; results were compared with proposed formula, refer to Table 5.

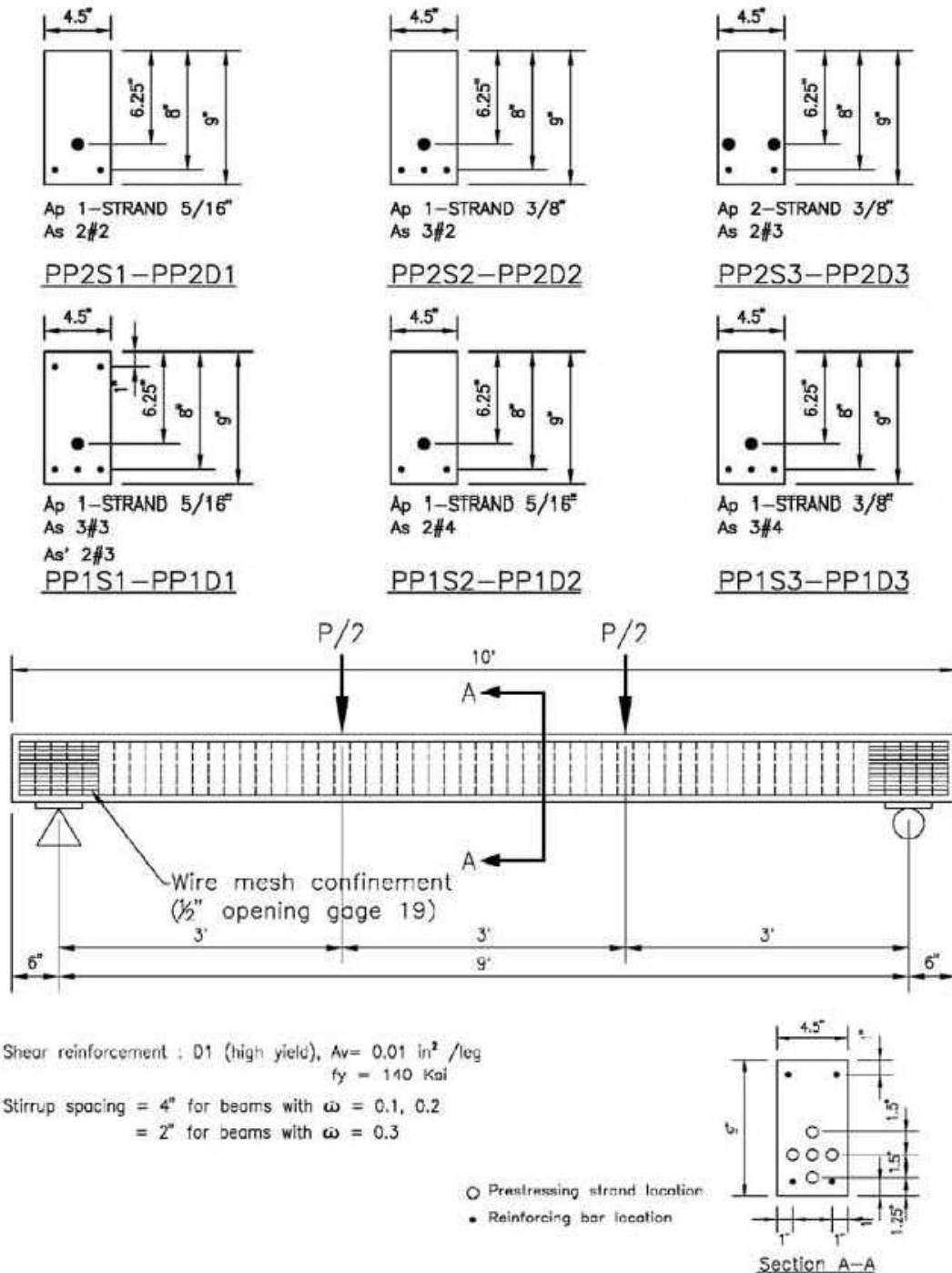


Figure 13: Beams details of test conducted by A.E. Namman and M.H. Harajli

4. Proposed formula for effective inertia and discussion

Table 5 shows a comparison of crack widths based on results of experimental tests, previous experimental test by A.E. Namman and M.H. Harajli [7] and formulas suggested by others [2], [3], [5] and [6]. It is clear that a formula given by Eurocode 2 [4] is the most accurate but it needs modification to consider PPR by multiplying the equation by a factor $\psi=1.40$ for $\text{PPR} \geq 0.5$ and $\psi=1.0$ for $\text{PPR} < 0.5$.

Table 5: Comparison of crack width using proposed formula and other methods

| BEAM | MAXIMUM CRACK WIDTH (mm) DUE TO MAXIMUM SERVICE LOAD | | | | | | | | |
|-------|--|------------------|---------------------|-------------------------|--------------------------|------------------------|---------------------------|-------------------------|----------------------------|
| | Actual | Proposed formula | Eurocode BS-EN-1991 | Gergely and Lutz (1968) | Nawy and Potyondy (1971) | Nawy and Chiang (1980) | Martino and Nilson (1979) | Meier and Gerely (1981) | Egyptian code ECP 203 2018 |
| S1 | 0.40 | 0.41 | 0.29 | 0.27 | 0.17 | 0.60 | 0.26 | 0.84 | 0.44 |
| S2 | 0.40 | 0.42 | 0.30 | 0.23 | 0.16 | 0.40 | 0.26 | 0.86 | 0.31 |
| S3 | 0.35 | 0.28 | 0.28 | 0.24 | 0.14 | 0.41 | 0.24 | 0.81 | 0.24 |
| S4 | 0.32 | 0.27 | 0.27 | 0.21 | 0.14 | 0.34 | 0.24 | 0.80 | 0.23 |
| S5 | 0.30 | 0.28 | 0.28 | 0.26 | 0.15 | 0.44 | 0.25 | 0.81 | 0.24 |
| S6 | 0.30 | 0.30 | 0.30 | 0.25 | 0.15 | 0.44 | 0.25 | 0.85 | 0.25 |
| S7 | 0.30 | 0.28 | 0.28 | 0.22 | 0.15 | 0.36 | 0.25 | 0.84 | 0.27 |
| S8 | 0.30 | 0.27 | 0.27 | 0.21 | 0.15 | 0.34 | 0.25 | 0.81 | 0.26 |
| S9 | 0.40 | 0.41 | 0.41 | 0.36 | 0.15 | 0.59 | 0.42 | 1.53 | 0.26 |
| PP1S1 | 0.26 | 0.26 | 0.26 | 0.16 | 0.15 | 0.27 | 0.22 | 0.93 | 0.32 |
| PP1S2 | 0.28 | 0.25 | 0.25 | 0.14 | 0.12 | 0.24 | 0.19 | 0.81 | 0.27 |
| PP1S3 | 0.21 | 0.24 | 0.24 | 0.13 | 0.12 | 0.16 | 0.20 | 0.87 | 0.25 |
| PP2S1 | 0.35 | 0.27 | 0.19 | 0.80 | 0.14 | 0.66 | 0.21 | 0.84 | 0.61 |
| PP2S2 | 0.35 | 0.31 | 0.22 | 0.15 | 0.12 | 0.38 | 0.20 | 0.79 | 0.42 |
| PP2S3 | 0.36 | 0.39 | 0.28 | 0.19 | 0.17 | 0.49 | 0.23 | 1.06 | 0.37 |

5. Conclusion

Based on results of tested beams and results of previous tests, the following conclusions can be deduced:

- j. Proposed formula gives acceptable results with maximum difference around 20%.
- k. PPR (consequently tension stress in reinforcement) is the most effective factor for maximum crack width, number of crack and crack spacing.
- l. PPR value between 0.30 and 0.4 is recommended for non-severe exposure.
- m. PPR more than 0.40 needs additional reinforcement for control of crack width.
- n. Prestressing level is inversely proportionate with ductility, and engineering judgment is required to benefit from enhancement of crack control and the required ductility level.
- o. Further studies are recommended for studying the effect of above mentioned variables with high strength concrete.

REFERENCES

- Naaman, A. E. (2022). *Prestressed Concrete Analysis and Design: Fundamentals*. Techno Press 3000.
- American Concrete Institute. (2015). *Building code requirements for structural concrete (Aci 318M-14): An Aci Standard: Commentary on building code requirements for structural concrete (Aci 318M-14)*.
- Precast/Prestressed Concrete Institute. (2010). *Pci Design Handbook: Precast and prestressed concrete*.
- British Standards Institution. (2004). *Eurocode 2: Design of concrete structures*.
- Arab Republic of Egypt Ministry of Housing, Utilities and Urban Communities Housing and Building National Research Centre. (2018). *Egyptian Code for Design and Construction of Concrete Structures*.
- American Concrete Institute. (2000). *State-of-the-art report on partially prestressed concrete*.
- Harajli, M. H., & Naaman, A. E. (1987). *Deformation and cracking of partially prestressed concrete beams under static and cyclic fatigue loading*. University Microfilms International.
- Arab Republic of Egypt Ministry of Housing, Utilities and Urban Communities Housing and Building National Research Centre. (2020). *Egyptian Code for Design and Construction of Concrete Structures*.
- American Concrete Institute. (2016). *Guide to estimating prestress loss*.
- American Concrete Institute. (2001). *Control of Cracking in Concrete Structures*.